

AN ELECTRIC FIELD SENSOR BASED ON A SHORT MONOPOLE ANTENNA

S.Y. Karelin, I.I. Magda, V.S. Mukhin

National Science Center “Kharkov Institute of Physics and Technology”, Kharkov, Ukraine

E-mail: magda@kipt.kharkov.ua

Discussed in the paper is application of an E-field probe in the form of a short monopole antenna (a D-dot-like configuration) for receiving short pulsed signals. Several numerical experiments have permitted suggesting recommendations as for implementing sensors with a uniform spectral response. Versions of the sensor configuration, suitable for operation with short pulsed signals with complex spectrum in the range of 0.5 to 3 GHz are considered, and results of probe calibrations presented.

PACS: 41.60, 84.30, 84.37

INTRODUCTION

To measure characteristics of ultra short pulsed (USP) electromagnetic signals, a variety of ultra-wideband (UWB) antennas can be applied, on the condition that their transient response should be of sufficiently short duration. All of them can be categorized either as nonresonant traveling wave or electrically short antennas. UWB antennas of the first type, capable of receiving USP signals without significant waveform distortions are represented, *e.g.* by the TEM horn. That is characterized by a frequency independent input impedance and ability to conserve the initial modal content of the transferred signal through the entire transmission length. By having a good impedance match design both at the aperture of the antenna and the output interface its output voltage waveform is identical to the incident E field. Meanwhile, a fundamental condition allowing for undistorted reception of pulsed signals of duration t_p is the requirement that the electric length L of the TEM horn is sufficiently large, $L > 2t_p c$, where c stands for the speed of light in the horn (possibly, filled with some medium). Unfortunately, in some cases the size L may prove unacceptably large because of a large t_p of the pulse.

An alternative to the TEM horn as a device for receiving pulsed electromagnetic signals with arbitrarily short width t_p may be a short monopole (SM), *i.e.* a non-symmetrical rod antenna known as the D-dot sensor, or DDS [1]. In contrast to the traveling wave antenna, the characteristic size of the DDS, namely $L \ll \lambda$ suggests a capacitive character for its input impedance, hence the signal at the output is proportional to the time derivative of the pulse's electric field strength E at the receiving location. Also, the response function of the DDS may happen frequency dependent, so generally, the DDS requires calibration through the operating frequency band. Despite the inconveniencies associated with these additional signal treatment procedures, the interest toward the DDS as an electric field sensor for USP signals (see, for instance, the recent paper on radiation sources of short, complex spectrum pulses [2]).

The present paper is dedicated to a study of performance characteristics of DDS and calibration thereof within a numerical experiment. The USP signals were formed in a nonlinear transmission line involving a gyrotropic medium. The appropriate waveforms appeared as decaying oscillatory ('sinusoidal') signatures with varying lengths of the quasiperiod and varying number of oscillations over the total pulse length [2]. We have sought an optimum structure and design of the sensor for minimizing distortions in the measured signals.

ISSN 1562-6016. BAHT. 2018. №4(116)

1. DETAILS OF THE NUMERICAL EXPERIMENT

The 3D numerical experimentation was carried out on the CST MW Studio platform [3]. The objects of study were versions of D-dot-like field sensors in a transmission line, differing in the configuration of their electrodes. A vertically polarized electromagnetic pulsed plane wave of a specific strength of its electric component was formed in the operating space. Each of the UWB pulsed signals showed the time behavior of a decaying sinusoidal form with a total number of oscillation periods, T , about 10 (Fig. 1). When interpreting the results, the time-domain description of the waveforms was confronted with a simplified frequency domain representation where a unique frequency estimate was obtained from the duration of the first quasiperiod T_1 , $f_0 = T_1^{-1}$. This magnitude varied from one experiment to another between 0.5 and 3 GHz, and the fractional spectral line width from 0.3 to 0.15.

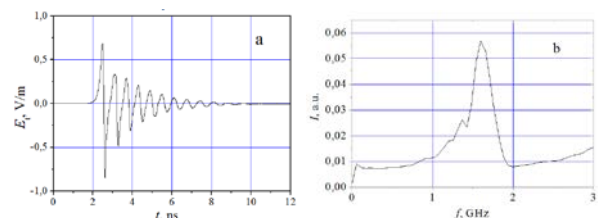


Fig. 1. Initial E-field waveform and spectrum

The electromagnetic wave field as described acted on the DDS in the form of a vertically oriented short monopole, plus a horizontally extended 'ground' electrode (GE). For each of the DDS structures analyzed, the condition that the monopole length h should be small compared with the shortest wavelength in the pulse spectrum ($h \ll \lambda_{0 \text{ MIN}}$) was satisfied.

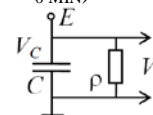


Fig. 2. DDS: A simplified equivalent circuit diagram

Fig. 2 shows a simplified equivalent electric circuit of the DDS. The short monopole is represented as a capacitor C to be charged inductively from the electric component $E(t)$ of the incident electromagnetic wave. The voltage across terminals of the capacitor-antenna, induced under optimal orientation conditions with respect to the E -field vector, is proportional to the magnitude of E and the effective antenna height h_A [4]

$$V_C(t) = h_A \cdot E(t). \quad (1)$$

The measuring circuit connected to C carries the current $i_C(t)$ whose magnitude is determined by the cable impedance ρ . Thus, the voltage formed at the cable output is

$$V(t) = i_C(t) \cdot \rho = \rho \cdot C \cdot dV_C(t)/dt. \quad (2)$$

Finally, we obtain the expression for the output voltage

$$V(t) = h_A \rho \cdot C \cdot dE(t)/dt, \quad (3)$$

from where it is obvious the necessity to integrating on time the output signal $V(t)$ for obtaining the electric field waveform $E(t)$, and also the DDS transmission factor $K = V/E$ dependence on frequency

$$K \approx h_A \rho \cdot C / \tau, \quad (4)$$

where τ is the constant of integration.

It is worthily to note that the effective antenna height h_A in (1) is a constant only when the spectral composition of the receiving EMW is invariable, e.g. when the impulse waveform does not change. This is not correct in general, because complex geometry of the DDS electrodes results in appearance in (1) an additional dependence on time (frequency), $h_A \rightarrow h_A(t-t')$. Taking into account that the DDS monopole height is small, $h \ll \lambda_{\text{MIN}} \approx 10$ cm, the time (frequency) dependence of h_A relates basically to the ground electrode geometry. Thus, the use of DDS for measurements the signals with complex spectral composition demands for providing an additional procedure – the probe calibration within the operation frequency band.

2. THE PROBE INVESTIGATION

Several modifications of DDS were considered. Their GE were specific for real experiment: (1) a wide plane disc with a coaxial vertical link imitating the outgoing signal line; (2) a wide-diameter hemisphere covering the vertical coaxial link; (3) a small disk with minimal the vertical coaxial link; (4) a small disk with the horizontal coaxial link.

The DDS-1 design (Fig. 3) was a vertical coaxial cable, in which the internal electrode was a short monopole of height h , and the outer electrode with its edges connected together in the center of a horizontally oriented metal disk forming a wide GP. The invariable dimensions in the DDS-1 design were: $h = 0.5$ cm, $d_1 = 0.25$ cm, $d_2 = 1$ cm, $h_1 = 5$ cm, and $h_2 = 0.25$ cm while the GP diameter d_3 was unchanged.

In the numerical experiment, an independent recording of the vertical component of the electric field strength $E(t)$ ($E_M = 0.8$ V/m) near the antenna (Fig. 4,a), and the signal $V(t)$ at the cable output (Fig. 4,b) were carried out.

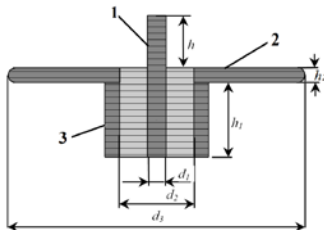


Fig. 3. Design of DDS-1. 1 – short monopole electrode; 2 – ground electrode; 3 – coaxial cable

Then the probe output signal was numerically integrated (Fig.4,c). Based on the comparison of the signals Fig. 4,a,c the transmission factor of the sensor K was determined. For example, the transmission factor of DDS-1 with $d_3 = 80$ cm was $K_1 = 0.82 \cdot 10^{-4}$ m.

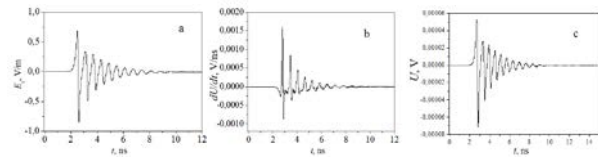


Fig. 4. The data used for DDS calibration. a – electric field strength near DDS; b – recorded output signal; c – integrated output signal. $E_M = 0.8$ V/m

Numerical experiments demonstrated variations of the DDS-1 output signal waveform depending on the value of d_3 , indicating the importance of the diffraction effects (spatial resonances) possible within the frequency range of the operating signal (see Fig. 1) DDS-1 was tested with a signal with the fixed-frequency harmonic component (in this case, $f_0 = 1.6$ GHz). Fig. 5 shows the output signal waveforms (after integrating and accounting for the transmission factor), depending on the GP diameter d_3 . As it can be seen, variation of the GP diameter d_3 produced various distortions of the pulse shape. The greatest output signal amplitude and waveform distortions were observed at smaller GP diameters 4 cm $< d_3 < 6$ cm. The waveform distortions appeared greater with the d_3 increase to 10 cm. But at the diameter further increase up to ~ 20 cm distortions became significantly smaller and disappeared at $d_3 > 40$ cm. Simultaneously, for $d_3 > 20$ cm, the signal output amplitude stabilized.

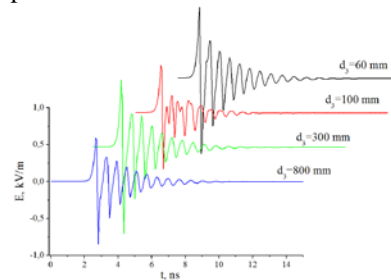


Fig. 5. The DDS-1 output signal waveforms for different GE diameters, $E_M = 0.8$ V/m

The obtained results become clear if we take into account the central frequency of the regular component in the irradiating impulse ~ 1.6 GHz ($\lambda_0 = 18.5$ cm). In this case, the distance to the GP disk edge, at which significant distortion of the waveform are present, corresponds to $d_3 = 10 \dots 20$ cm $\approx \lambda_0$. Accordingly, for $d_3 > \lambda_0$, the resonant effects are sufficiently attenuated, and the signal distortions decreased. It is interesting to note that the range of values $d_3 < \lambda_0$ (30...60 cm), is also characterized by small distortions in the waveform, and by significant increase of K (up to 1.5 times). This effect is obviously due to the insufficient shielding of the vertical coaxial link located at the bottom of the GP. In this case, the vertical orientation of the link could contribute to an increase in the effective height of the antenna resulting in somewhat increase of $V(t)$.

Thus, the range of d_3 values, at which a good “shielding” of the outgoing coaxial line was provided and the spatial resonances corresponding to the chosen operating spectrum were not observed, corresponded to 20...30 cm, i.e. $d_3 \geq c/f_0$. On the other hand, an excessive increase in d_3 creates certain inconveniences when using the sensor. Therefore, the value $d_3 = 20 \dots 30$ cm is optimal for a signal with a selected frequency of 1.6 GHz.

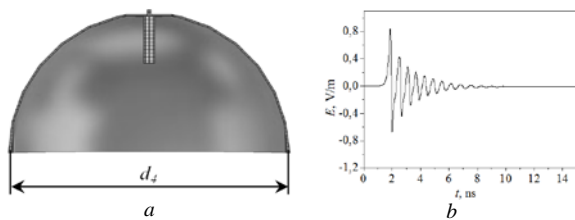


Fig. 6. The DDS-2 configuration (a), and output signal (b), $E_M = 0.8 \text{ V/m}$

As can be seen, “shielding” of the output coaxial line due to an increase in the transverse dimension of the sensor's $d_3 > \lambda_0$, when the appearance of dimensional resonances decreases, is one of the ways to minimize distortions of the received signal. Another way to solve the problem is the use of the GE with an optimal d_3 and bent edges, which provide shielding for the coaxial vertical link. This approach was implemented in the design of DDS-2, having the GE with $d_3 = 30 \text{ cm}$ and hemispherical shape (Fig. 6,a). Fig. 6,b shows the signal registered by DDS-2, which has small distortions in shape.

The possibility to obtaining a minimal distortion of the signal waveform by eliminating the influence of the coaxial vertical line was verified in the third modification of the probe (DDS-3), where the height of the coaxial line h was minimal (Fig. 7,a). The GE dimensions were also chosen as small as possible and corresponded to the conditions:

$$h_1 \ll d_3 < \lambda_{0 \text{ MIN}}. \quad (5)$$

DDS-3 had the following dimensions of the GE: $d_3 = 6 \text{ cm}$, and $h_2 = 0.25 \text{ cm}$. As it can be seen in Fig. 7, b, the signal detected by DDS-3 was practically free of distortion. This result indicates that operation with the signals with complex spectral content requires using a sensor with dimensions satisfying the condition (5).

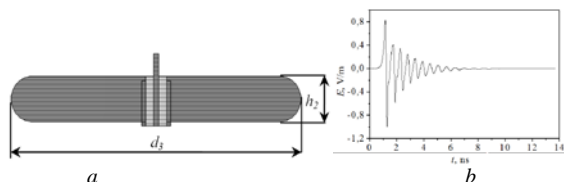


Fig. 7. The DDS-3 design (a), and its output signal (b), $E_M = 0.8 \text{ V/m}$

It was noted earlier that the capacitive nature of the SM and the spatial non-uniformity of the GE are both the causes of the frequency dependence of the DDS response function. In our case, this manifested itself in the distortion of the waveform of the received signal. To clarify the impact of geometric characteristics of the DDS under study on the shape of the output signals, the sensors were tested using a quasi-harmonic signal within the frequency range corresponding to the above-mentioned 0.5 to 3 GHz operating frequency. The results of the measured E field of a quasi-harmonic signal obtained for various DDS are presented in Fig. 8. As can be seen, the DDS-1 and DDS-2 sensors (curves 1-4) have significant (~20...25%) non-uniformity of the frequency dependence $V = V(f_0)$. In DDS-3 (curve 5) with the dimensions of the electrodes meeting the condition (5), the frequency non-uniformity does not exceed of ~15%, which is confirmed by the observation of smaller signal distortions than in DDS-1 and DDS-2.

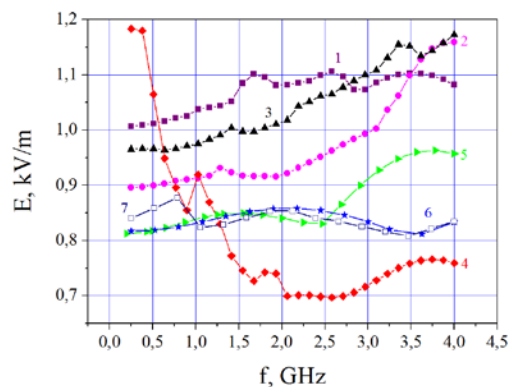


Fig. 8. Results of DDS tests using a quasi-harmonic signal. 1, 2, 3 – DDS-1 ($d_3 = 6, 10$ and 30 cm); 4 – DDS-2; 5 – DDS-3; 6 – DDS-4 ($l = 2 \text{ cm}$); 7 – DDS-4 ($l = 10 \text{ cm}$)

However, due to the absence of the output signal cable, the DDS-3 can not be used in practice. Therefore, a more realistic design of the DDS-4 with the coaxial link was considered, Fig. 9. This design used a small-diameter coaxial cable, which was oriented horizontally to reduce the electromagnetic coupling to the vertically polarized EMW. Moreover, to reduce the level of precursor-signals it was turned opposite to the direction of arrival of the EMW.

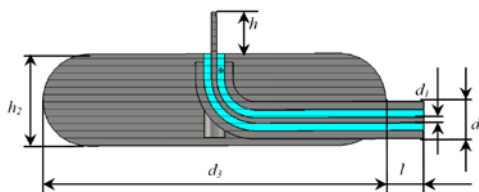


Fig. 9. DDS-4 with a horizontally oriented signal cable

The characteristic dimensions of the DDS-4 are: $h = 0.5 \text{ cm}$; $d_2 = 0.25 \text{ cm}$; $d_3 = 3 \text{ cm}$; $h_2 = 1 \text{ cm}$. Two variants of the DDS-4 with different length of the coaxial link ($l = 2 \text{ cm}$ and 10 cm) were tested. These two sensors, like the DDS-3, did not practically distort the received signal, and their amplitude-frequency characteristics (Fig. 8, curves 6 and 7) had minimal nonuniformities, 3.6 and 7%, respectively.

3. DISCUSSION

In the study of broadband DDS, conducted on the basis of numerical simulation, several sensor designs for receiving SKD signals with a complex spectral composition are considered. It is known the use of DDS for recording free space transient signals of subnanosecond width [1, 5]. The spectrum of such signals is enriched, mainly by HF components, which are almost not distorted by a sensor having a small-size GE. Generally, signal distortions are formed as a result of interference of its main part and reflections from the inhomogeneities of the GE, from the adjacent elements (for example, signal cables) or from surrounding radio-contrast objects. If the scattering element is removed from the SM by a distance z , the reflected signal lags behind the main pulse for a sufficiently large time of $\sim 2z/c$. This corresponds to the appearance of a LF component in the signal spectrum. For example, at receiving a sub-ns signal, a DDS with the $d_3 > 20 \text{ cm}$ will form a response from the GE edge, separated from the beginning of

pulse by a time of about 1 ns. This "tail" can easily be filtered by a time gate. Accordingly, the initial spectrum of the USP signal having a maximum in the region of the frontal frequencies ($f = 0.35/t_R$), will be enriched at the sensor output with the 1 GHz or less components, which can also be easily filtered.

Quite a different situation arises when recording signals having a complex waveform and width, comparable to or exceeding the electric length of the GE $\sim 2d/s$. In our case, the signal width is of 12...15 ns and includes a damped harmonic component with $f = 0.5...3$ GHz. Accordingly, any reflection from the edge or inhomogeneity of the GE falls into the range of the fundamental frequency of the signal spectrum and substantially disturbs the waveform. Obviously, the solution to our problem is related to a principal reduction in the GE dimension, so that possible reflections will be outside the operation frequency band.

The results of numerical experiments carried out with DDS variants can be compared with formula (4), which reflects the relationship between the amplitude and shape of the output signal and the design characteristics of the sensor. Obviously, the transmission factor of the sensor $K = V/E$ depends only on the magnitude of the two components: the effective height of the sensor as an antenna, h_A and the capacitance of the monopole to the ground electrode, $K(\rho = \text{const}) \sim h_A C$. Both these quantities are determined by the geometric features of the DDS as a whole.

Some DDS with coaxial vertical link demonstrated characteristic large amplitudes of the output signal compared to the signals of flat DDS. The vertical link of DDS-1 and DDS-2 increased the effective antenna height h_A and, correspondingly, increased the transmission factor (4).

In view of the same relation, a larger transmission coefficient is also characteristic for DDS with a large diameter of the GE, since the amplification of the short monopole antenna is proportional to the capacitance of the SM to the ground. Because of this, DDSs having large d_3 showed a rise in the amplitude of the HF components of the signal (curves 2 and 3). Accordingly, the transmission factor of the DDS-1 with a small-diameter GE was characterized by a weakening of the HF components (curve 1).

Similarly to a small-diameter DDS-1, the remote areas of the DDS-2 ground electrode with a hemispherical shape produced smaller amplification of the HF signal components. Their capacitive coupling with the periphery was attenuated by the GE curvature (curve 4). In

this case, DDS-2 clearly demonstrated a LF resonance – the GE vertical arrangement caused a rise in h_A .

Small-diameter sensors DDS-3 and DDS-4 formed the output signal with significantly smaller amplitude than DDS with large d (curves 5, 6 and 7). Since the dimensions of these sensors were far from resonance values, their spectra were generally uniform in frequency. The exception was represented by DDS-4 (curve 7) having a long horizontal coaxial link. Due to its small outer diameter of the cable, this link produced weak resonant increase of the LF components of the signal spectrum.

CONCLUSIONS

The results of the numerical studying a sensor recording USP signals with a complex spectral composition including a harmonic component were used to substantiate the possibility to obtain a uniform frequency response in the frequency range 0.5...3 GHz. The results of the numerical studying a sensor recording USP signals with a complex spectral composition including a harmonic component have been used to substantiate the possibility to obtain a uniform frequency response in the frequency range 0.5...3 GHz. It has been shown that the sensor sensitivity is determined by the features of its design – the effective height of the device as an antenna, and the electric capacitance of the monopole to the earth electrode. The degree of distortion of the received USP signal waveform depends on the fulfillment of the condition for the DDS electrode dimensions, $h \ll d_3 < \lambda_{0 \text{ MIN}}$, which means the absence of resonances within the signal spectrum.

REFERENCES

1. A.A. Agry, R.A. Schill. Calibration of Electromagnetic Dot Sensor. Part 1 // *IEEE Sensors Journal*. 2014, v. 14, № 9, p. 3101-3118.
2. J.-W. Ahn, S.Y. Karelin, V.B. Krasovitsky, H.-O. Kwon, I.I. Magda, V.S. Mukhin, O.G. Melezhik, V.G. Sinitsin. Wideband RF Radiation from a Nonlinear Transmission Line with a Pre-magnetized Ferromagnetic Core // *Journal of Magnetism*. 2016, v. 21, № 3, p. 450-459.
3. <http://cst-microwave-studio.software.com>.
4. F. Sonnemann. Experimental and numerical analysis on PCB coupling in non-uniform field environment. // *Advances in Radio Science*. 2004, № 2, p. 83-86.
5. T.R. Johnk, A.R. Ondrejka. Time-Domain Calibrations of D-Dot Sensors // *NIST Technical Note 1392*. Boulder, Colorado. 1998, 21 p.

Article received 04.06.2018

ДАТЧИК ЭЛЕКТРИЧЕСКОГО ПОЛЯ НА ОСНОВЕ КОРОТКОЙ НЕСИММЕТРИЧНОЙ АНТЕННЫ

С.Ю. Карелин, И.И. Магда, В.С. Мухин

Рассматривается применение зонда Е-поля в виде короткой несимметричной антенны, известного как D-dot зонд, для регистрации излучаемых импульсных электромагнитных сигналов сверхкороткой длительности. Численные эксперименты позволили предложить рекомендации, касающиеся геометрических особенностей датчика с равномерным спектральным откликом. Рассмотрены варианты конфигурации датчика, соответствующие работе с короткоимпульсными сигналами со сложным спектром в области частот от 0,5...3 ГГц, и представлены результаты его калибровки.

ДАТЧИК ЕЛЕКТРИЧНОГО ПОЛЯ НА ОСНОВІ КОРОТКОЇ НЕСИМЕТРИЧНОЇ АНТЕНИ

С.Ю. Карелін, І.І. Магда, В.С. Мухін

Розглядається застосування зонда Е-поля у вигляді короткої несиметричної антени, відомого як D-dot зонд, для реєстрації випромінюваних імпульсних електромагнітних сигналів надкороткої тривалості. Чисельні експерименти дозволили запропонувати рекомендації, що стосуються геометричних особливостей датчика з рівномірним спектральним відгуком. Розглянуто варіанти конфігурації датчика, що відповідають роботі з короткоімпульсними сигналами із складним спектром в області частот від 0,5 ... 3 ГГц, і представлені результати його калібрування.